

# Multi-organ Segmentation by Minimization of Higher-order Energy for CT Boundary

Asuka Okagawa<sup>1,2</sup>, Yuji Oyamada<sup>1,2</sup>, Yoshihiko Mochizuki<sup>1,2</sup>, and Hiroshi Ishikawa<sup>1,2</sup>

<sup>1</sup>Department of Computer Science and Engineering, Waseda University

<sup>2</sup>JST CREST

## Abstract

*In medical image analysis, segmentation of medical images such as Computed Tomography (CT) volumetric images is necessary for further medical image analysis and computer aided intervention. We propose a method for medical image segmentation by higher-order energy minimization. Specifically, we introduce a higher-order term that describes the continuity around the edge points of a CT image. The parameters of the energy terms are determined according to various conditional probabilities learned from sample data with the ground truth. Then we minimize the energy using graph cuts and evaluate the effectiveness of the introduction of the term into the traditional energy.*

## 1 Introduction

Image segmentation for a computed tomography (CT) data is one of the major topics in medical image analysis. CT data may be a two or three dimensional image, or volume, of the radiodensity, known as CT number, which differs for different objects in the scanned body. This would be useful for diagnosis or assist for surgical operation, and there is a great demand to extract the region of objects automatically by image processing such as segmentation.

Many methods for medical image segmentation have been proposed [1]. To segment multiple organs of volumetric CT image simultaneously [2][3][4] is still a challenging task. One formulation of the problem is to express the segmentation as a labeling for each voxel and to solve by energy minimization, which seeks the global minimum of a energy function measuring the inaccuracy of estimates. A class of the minimization problem can effectively solved by graph-cut based methods. Although the order of energy function in the class, which describes the degree of dependency among voxels, has been limited to 1, this limitation has been overcome in recent works [5, 6, 7] that convert a higher-order energy to the second-order one. A higher-order energy enables us to express complex constraints among multiple organs or widely spanning structure[8]. However, defining the effective energy applicable to specific problems is still a challenging task.

In this paper, we analyze the relationship between the probabilistic atlas, the ground truth of segmentation, and the distribution of CT values, then propose a new energy function with higher-order terms describing a constraint on wider region. Specifically, we introduce a higher-order term that describes the continuity around the edge points of a CT image. We learn various conditional probabilities to determine the parameters of the energy terms, and then minimize the energy

using graph cuts. We then evaluate the effectiveness of the introduction of the term into the traditional energy.

## 2 Medical Image Segmentation

Let  $\mathcal{V} \subset \mathbb{Z}^3$  be a regular lattice of voxels,  $X: \mathcal{V} \rightarrow \mathbb{R}$  an 3D CT image,  $\mathcal{L} = \{0, 1, \dots, M\}$  a set of labels, each designating an organ, except that the label 0 designates the background. For input image  $X$  a labeling  $L: \mathcal{V} \rightarrow \mathcal{L}$  which assigns a label  $L_v \in \mathcal{L}$  to each voxel  $v \in \mathcal{V}$  is called a segmentation of  $X$ .

### 2.1 Energy minimization

The problem to find the best segmentation  $L$  of an image can be formulated as the minimization of the energy function  $E(L)$  such as

$$E(L) = \sum_{C \in \mathcal{C}} f_C(L_C). \quad (1)$$

Here,  $\mathcal{C}$  is a set of cliques which are subsets of voxels in  $\mathcal{V}$  and  $f_C$  a potential function defined over the voxels in a clique  $C$ .

For segmentation of medical images the energy function is practically defined as follows.

$$\begin{aligned} E(L; X) &= w_A E_A(L) \\ &+ w_D E_D(L; X) \\ &+ w_S E_S(L; X), \end{aligned} \quad (2)$$

where  $E_A(L)$ ,  $E_D(L; X)$ , and  $E_S(L; X)$  are an atlas, data, and smoothness terms, respectively, and  $w_A$ ,  $w_D$ , and  $w_S$  are weights corresponding to the three terms.

**Atlas term** Atlas term is a potential dependent to the location of a voxel, which is defined by a probability  $\Pr(L)$  for each voxel. This is called probabilistic atlas and can be constructed with a set of training data with atlases labelled manually. Thus, this term is defined for the cliques  $\mathcal{V}$  as

$$E_A(L) = \sum_{v \in \mathcal{V}} -\ln \Pr(L_v). \quad (3)$$

**Data term** Data term determines which label should be assigned according to the probability of occurrence of CT value for each label. The probability can be inferred from the training dataset and the potential function is defined as

$$E_D(L; X) = \sum_{v \in \mathcal{V}} -\ln \Pr(X_v | L_v). \quad (4)$$

**Smoothness term** The region of an organ is connected without fragmentation. Smoothness term constrains two neighboring labels should be the same. Thus the potential function is defined for the clique  $\mathcal{N} \subset \mathcal{V} \times \mathcal{V}$  which consists all pairs of the neighboring voxels as follows:

$$E_S(L; X) = \sum_{(u,v) \in \mathcal{N}} h_{u,v}(L_u, L_v, X_u, X_v), \quad (5)$$

where  $h$  is Potts potential defined as

$$h_{u,v}(L_u, L_v, X_u, X_v) = \begin{cases} 0 & \text{if } L_u = L_v, \\ (|X_u - X_v| + 1)^{-1} & \text{otherwise.} \end{cases} \quad (6)$$

The energy function for multiple labels can be minimized approximately by using the fusion-move strategy [9]. Fusion-move algorithm will generate the labeling with lower energy than the current labeling by giving a labeling called the proposal. In our problem, due to connectivity of the region of organs, we can give a uniform labeling, which assigns a certain label for all voxels, as a proposal repeatedly for each label.

## 2.2 Higher-order Energy

For a clique  $C$ ,  $|C|-1$  is called the *order* of the clique and the potential  $f_C$ . The order of energy function is the maximum order of the potentials in it. An energy whose order is greater than 2 is called a higher-order energy.

Higher-order potentials depend on more than 2 voxels. Such higher-order dependency should be useful to describe constraints among some organs.

Until recently the order of energy which can be solved by QPBO[10] is limited to 1. Some algorithms to convert the function of any order to that of the first order have been proposed [5, 7]. This enables us to use any higher-order energy to describe more complicated conditions.

## 3 Proposed method

Segmentation result of the energy function with data, atlas and smoothness terms is sometimes inaccurate. Figure 1 shows an result, in which some organs are not properly segmented. In this example the left part of the liver is incorrectly labelled as another organ even though the CT values in the region of the liver are roughly constant and there seems no apparent changes in it. The atlas and data terms have just information of a voxel of each position, the smoothness terms only affect a pair of labels which are different each other. In order to give a constraint around the edge points, observation of more than 2 voxels is needed. This can be achieved by incorporating a higher-order potential into the energy function.

We can find the boundary of intensity in the CT image shown in Fig. 1. The boundary can be detected as a set of edge points whose gradient of the CT image is larger than a threshold, which can be detected by using some detection methods such as Canny edge detector [11]. Figure 1 shows the edges detected by three dimensional Canny detector in white, superimposed on

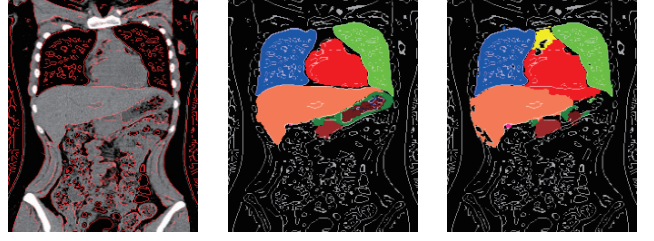


Figure 1. An example of poorly-segmented result for the liver. Left: the input CT image. Center: ground truth of segmentation. Right: segmentation result using data, atlas and smoothness terms. Lines in CT image and ground truth show the edge of CT values. The label for the liver is colored in pale orange.

the atlas. It can be seen that the organs are completely bounded by the edges. This implies that the label of an organ tends to be discontinued across the edge.

The discontinuity of labels across the edge should be encouraged for segmentation. However, the smoothness term does not work at the edge if the adjacent labels are the same. To express this we should observe along consecutive voxels if the labels exists uniformly and are discontinued on the edge.

In this paper, we propose a higher-order potential using the edge of intensity in the CT image. The potential would be conditioned by the existence of edges in the cliques, and depend on the some voxels to ensure the discontinuity around the edge. The proposed higher-order term  $E_H(L)$  is defined as follows. Let  $\mathcal{C}_n$  be the set of cliques for this potential, each of which consists with  $n$  continuous voxels in a line. Let  $\bar{X}$  be the edge image of  $X$ ,  $\bar{X}(v) = 1$  if  $v$  is on the edge point, 0 otherwise. We define the function to predicate if some edge points exist in a clique  $C$  as follows:

$$g(C; \bar{X}) = 1 - \prod_{v \in C} \bar{X}(v). \quad (7)$$

Then we define the proposed term as

$$E_H(L) = \sum_{C \in \mathcal{C}_n} f_C(L_C) \quad (8)$$

where

$$f_C(L_C) = \begin{cases} 0 & \text{if } g(C) = 0 \wedge (\exists l \in \mathcal{L}', \forall v \in C, L_v = l), \\ 1 & \text{otherwise,} \end{cases} \quad (9)$$

where  $\mathcal{L}' \subset \mathcal{L}$  is a selected organs which this potential affects.

Finally we define the energy function for segmentation as follows.

$$E(L; X) = w_A E_A(L) + w_D E_D(L; X) + w_S E_S(L; X) + w_H E_H(L), \quad (10)$$

where  $w_H$  is the weight for the higher-order term, if  $w_H = 0$ , the function is identical to the base energy function Eq. (2).

## 4 Experimental results

To evaluate the effect of the proposed higher-order term we compared the segmentation results between with and without the term. We use the dataset containing 76 non-contrast CT images. All images are pre-processed to reduce difference among individuals such as the body frame or alignment of organs, by registration with scaling and translation into  $209 \times 158 \times 258$  voxels in size. Each image has an atlas for 21 organs labelled manually. Due to the limited number of data, we use the leave-one-out validation for training and testing. The accuracy of segmentation results were evaluated by Jaccard index for non-background labels.

In this experiment, we focused on improving of the accuracy of the liver. We use the higher-order term with setting  $\mathcal{L}$  to the label of liver. The cliques used for the higher-order term is designed as the consecutive 6 voxels in x-direction, which define the 5th order potential. We placed the cliques in the limited region to avoid the untoward effect for the other organs. The region is determined according to the probabilistic atlas of liver.

The edge voxels for each image is detected by Canny edge detector [11] extended to the 3D image. Figure 1 show the edge voxels superimposed on the input CT image and the ground truth labeling. While the weights for non-higher-order term were  $w_A = w_D = 1$ ,  $w_S = 10$ , the weight for higher-order term is set to different values.

Table 1 shows the mean of Jaccard index of the segmentation results for  $w_H = 0$ , and between 0.4 and 1.2. The energy with  $w_H = 0$  is the base energy identical to Eq. (2). There is no remarkable improvement relative to the base energy. Table 2 shows the statistics for the worst 12 cases in terms of the Jaccard index by the base energy. The accuracy for worse cases are improved wholly.

Figure 2 show the results of three cases. From left to right, input CT images, ground truth, segmentation result without higher-order term, and result with higher-order term. The weights for the higher-order term are  $w_H = 1.5, 0.5, 0.5$ , respectively, which give the best JI scores for the liver. Figure 3 shows the results for different weights of the higher-order term. The region of liver extends with increasing the weight.

## 5 Conclusion

In this paper, we propose a higher-order energy for multi-organ segmentation that introduces a higher-order term that describes the continuity around the edge points of a CT image, we utilizing the boundary information of CT values and its discontinuity. In the experimental results, the accuracy is improved in some cases. As a future work the problem of robustness should be solved.

## Acknowledgement

This work was partially supported by KAKENHI 26108003 from JSPS as well as CREST from JST.

## References

- [1] A. Elnakib, G. Gimelfarb, J. Suri, and A. El-Baz, "Medical image segmentation: A brief survey," in *Multi Modality State-of-the-Art Medical Image Segmentation and Registration Methodologies*, pp. 1–39, Springer New York, 2011.
- [2] C. Chu, M. Oda, T. Kitasaka, K. Misawa, M. Fujiwara, Y. Hayashi, Y. Nimura, D. Rueckert, and K. Mori, "Multi-organ segmentation based on spatially-divided probabilistic atlas from 3d abdominal ct images," in *Medical Image Computing and Computer-Assisted Intervention (MICCAI)*, vol. 8150 of *Lecture Notes in Computer Science*, pp. 165–172, Springer Berlin Heidelberg, 2013.
- [3] M. G. Linguraru, J. A. Pura, V. Pamulapati, and R. M. Summers, "Statistical 4d graphs for multi-organ abdominal segmentation from multiphase ct," *Medical Image Analysis*, vol. 16, no. 4, pp. 904 – 914, 2012.
- [4] R. Wolz, C. Chu, K. Misawa, K. Mori, and D. Rueckert, "Multi-organ abdominal ct segmentation using hierarchically weighted subject-specific atlases," in *Medical Image Computing and Computer-Assisted Intervention (MICCAI)*, vol. 7510 of *Lecture Notes in Computer Science*, pp. 10–17, Springer Berlin Heidelberg, 2012.
- [5] H. Ishikawa, "Transformation of general binary mrf minimization to the first-order case," *IEEE Transactions on Pattern Analysis and Machine Intelligence*, vol. 33, pp. 1234–1249, June 2011.
- [6] A. Fix, A. Gruber, E. Boros, and R. Zabih, "A graph cut algorithm for higher-order markov random fields," in *2011 IEEE International Conference on Computer Vision (ICCV)*, pp. 1020–1027, Nov 2011.
- [7] H. Ishikawa, "Higher-order clique reduction without auxiliary variables," in *IEEE Conference on Computer Vision and Pattern Recognition, CVPR 2014*, pp. 1362–1369, 2014.
- [8] Y. Kitamura, Y. Li, W. Ito, and H. Ishikawa, "Coronary lumen and plaque segmentation from cta using higher-order shape prior," in *Medical Image Computing and Computer-Assisted Intervention (MICCAI)*, pp. 339–347, Springer, 2014.
- [9] V. Lempitsky, C. Rother, and A. Blake, "LogCut — efficient graph cut optimization for Markov random fields," in *ECCV2006*, pp. 269–282, 2006.
- [10] V. Kolmogorov and R. Zabih, "What energy functions can be minimized via graph cut?," *IEEE Transactions on Pattern Analysis and Machine Intelligence*, vol. 26, no. 2, pp. 147–159, 2004.
- [11] J. Canny, "A computational approach to edge detection," *IEEE Transactions on Pattern Analysis and Machine Intelligence*, no. 6, pp. 679–698, 1986.

Table 1. Mean Jaccard index for all cases. The energy with  $w_H = 0$  is corresponding to the base energy.

| $w_H$ | 0      | 0.4    | 0.5    | 0.6    | 0.7    | 0.8    | 0.9    | 1.0    | 1.1    | 1.2    |
|-------|--------|--------|--------|--------|--------|--------|--------|--------|--------|--------|
| all   | 0.7532 | 0.7514 | 0.7515 | 0.7509 | 0.7497 | 0.7483 | 0.7474 | 0.7452 | 0.7438 | 0.7423 |
| liver | 0.7714 | 0.7653 | 0.7653 | 0.7634 | 0.7603 | 0.7563 | 0.7536 | 0.7484 | 0.7442 | 0.7397 |

Table 2. Mean Jaccard index for the worst 12 cases. The energy with  $w_H = 0$  is corresponding to the base energy.

| $w_H$ | 0      | 0.4    | 0.5    | 0.6    | 0.7    | 0.8    | 0.9           | 1.0           | 1.1    | 1.2    |
|-------|--------|--------|--------|--------|--------|--------|---------------|---------------|--------|--------|
| all   | 0.6677 | 0.6701 | 0.6709 | 0.6713 | 0.6721 | 0.6721 | 0.6732        | <b>0.6740</b> | 0.6732 | 0.6730 |
| liver | 0.6780 | 0.6836 | 0.6853 | 0.6863 | 0.6870 | 0.6851 | <b>0.6872</b> | 0.6858        | 0.6831 | 0.6814 |

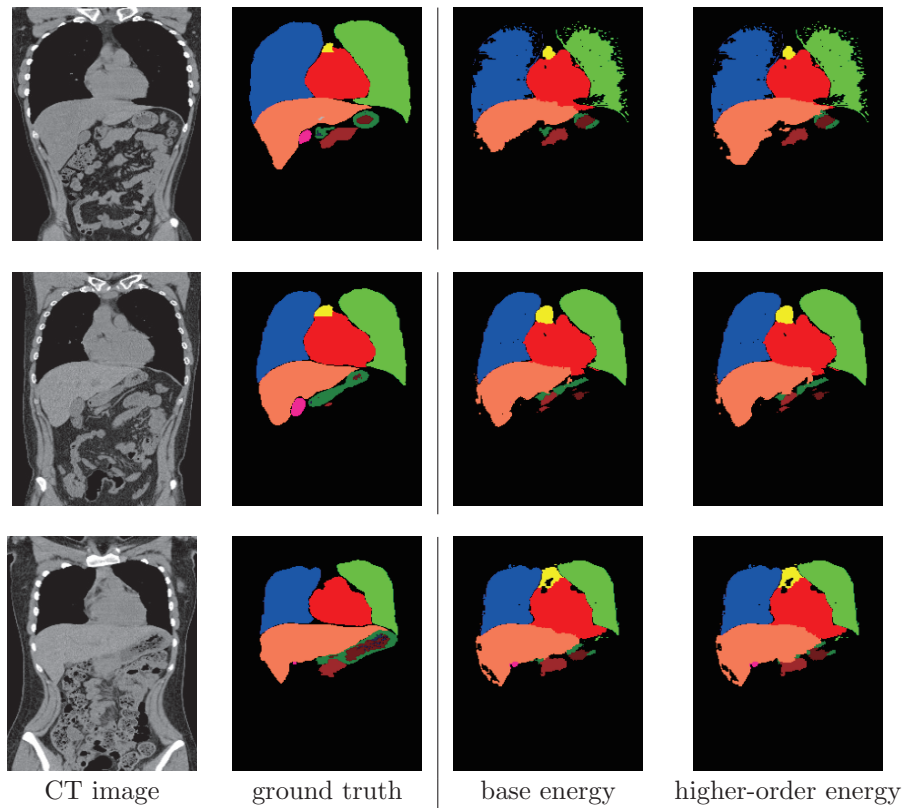


Figure 2. The best Segmentation results for three cases. The weights for the higher-order term are  $w_H = 1.5$ , 0.5, 0.5, respectively. From left to right, input CT images, ground truth, segmentation result without higher-order term, and result with higher-order term.

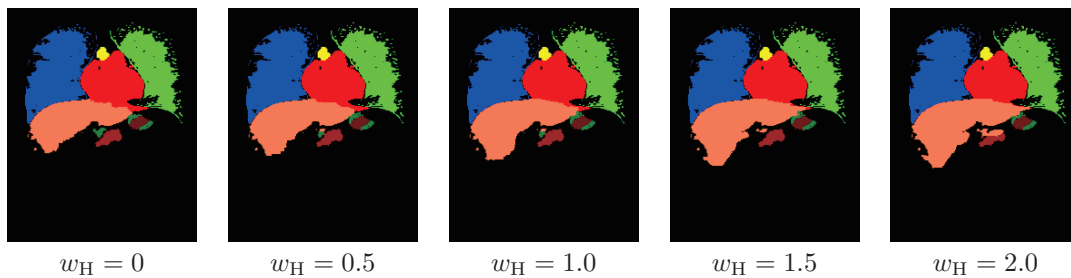


Figure 3. An example of segmentation results for different weight parameters.